MC-SCF Study of the Addition Reaction of the $^1\Delta_g$ Oxygen Molecule to Ethene

Glauco Tonachini,*[1a] H. Bernhard Schlegel,[1b] Fernando Bernardi,[1c] and Michael A. Robb[1d]

Contribution from the Istituto di Chimica Organica, Università di Torino, Torino, Italy, Department of Chemistry, Wayne State University, Detroit, Michigan 48202, Dipartimento di Chimica "G. Ciamician", Università di Bologna, Bologna, Italy, and Kings College, London, United Kingdom. *Received November 10, 1988*

Abstract: The potential energy hypersurface for the addition reaction of the singlet oxygen molecule and ethene has been studied at the MC-SCF level of theory, completely optimizing the geometries of the critical points and characterizing them as minima and first or higher order saddle points. The possibility of three kinds of attack to produce dioxetane has been considered: concerted [2 + 2] attacks with different geometrical approaches, attacks proceeding through species of diradicaloid nature, and an attack leading to peroxirane as a possible intermediate. The concerted paths are not viable, since the corresponding critical points are saddle points of order higher than 1. Two diradical paths exist and are defined by two transition structures (located at about 30 kcal mol^{-1} above the dissociation limit) and by distinct conformational minima of the peroxy diradical (located at about 18 kcal mol^{-1} above the dissociation limit), of which the gauche minimum can lead to dioxetane. Hence, the diradical pathway corresponds to a two-step mechanism. A peroxirane minimum is present on the surface, but a minimum energy path leading directly to it does not appear to exist: the peroxirane-like critical point of C_s symmetry is found to be a second-order saddle point and therefore does not correspond to a transition structure. Consequently, the peroxirane minimum seems to be reachable only passing through the gauche-diradical minimum.

The addition of the singlet oxygen molecule[2] to double bonds has been at the center of much experimental and theoretical work.[3a,b] These reactions fall into three main categories: (i) 1,2-addition to give dioxetanes; (ii) 1,3-addition (ene) reaction; (iii) 1,4-addition to form *endo*-peroxides (Scheme I).

These reactions are experimentally well-known and exploited in numerous syntheses. Not as well-known are the actual mechanisms of addition, and many (sometimes contrasting) hypotheses have been advanced. The present paper focuses on the addition of O_2 to one double bond to give dioxetanes.[3c,d] This reaction is sometimes also invoked as a first step in the ene mechanism.[3e] The main proposals for the mechanism of this reaction are shown in Chart I and include both concerted (with variable degrees of asynchronicity) and nonconcerted approaches: (1) a supra-supra attack (with possible charge transfer from ethene to a π^* orbital of O_2); (2) a supra-antara attack; (3) the involvement of a 1,4-diradical intermediate; (4) the involvement of a 1,4-amphoionic intermediate;[4] (5) the formation of an intermediate perepoxide.

The first four types of attack are conceivable for most [2 + 2] cycloadditions, while the last mode of attack (a kind of cheletropic reaction) is made possible by the presence of the oxygen lone pairs.

A detailed review of the experimental literature has been provided by Frimer.[3a] This literature is rather extensive, and evidence can be found for and against each of the mentioned mechanisms. Also various theoretical studies on this reaction have appeared, and their conclusions support different mechanisms.

Scheme I

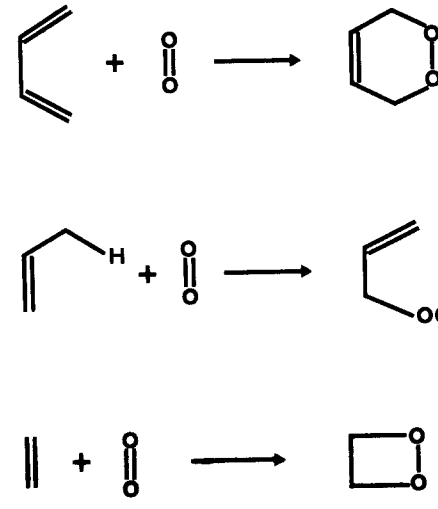

Chart I

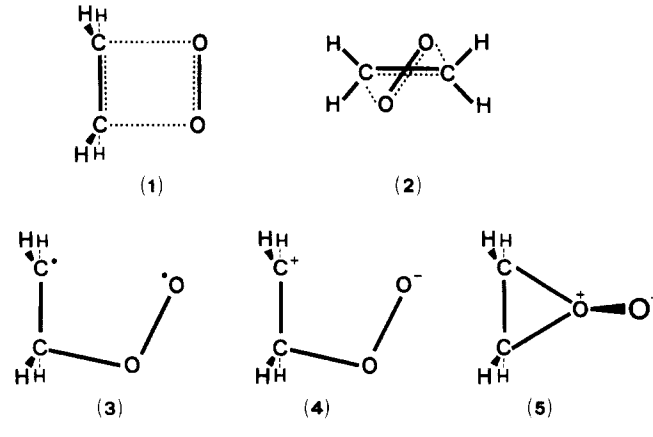

Some of the more important arguments are summarized below.

A concerted mechanism seems to be supported by studies focusing on the solvent response.[6a,b] In some cases, where the

(1) (a) Università di Torino (permanent address) and Wayne State University. (b) Wayne State University. (c) Università di Bologna. (d) Kings College.

(2) (a) Kearns, D. R. *Chem. Rev.* **1971**, *71*, 395-427. (b) Moss, B. J.; Goddard, W. A., III. *J. Chem. Phys.* **1975**, *63*, 3523-3531. (c) Moss, B. J.; Bobrowicz, F. W.; Goddard, W. A., III. *J. Chem. Phys.* **1975**, *63*, 4632-4639.

(3) (a) Frimer, A. A. *Chem. Rev.* **1979**, *79*, 359-387, and references therein. (b) Schaap, A. P.; Zaklika, K. A. In *Singlet Oxygen*; Wasserman, H. H., Murray, R. W., Eds.; Academic Press: New York, 1979; Chapter 6. (c) Bartlett, P. O.; Landis, M. E. *Ibid.* Chapter 7. (d) Adam, W. *Pure Appl. Chem.* **1980**, *52*, 2591-2608. (e) Stephenson, L. M.; Grdina, M. J.; Orphanopoulos, M. *Acc. Chem. Res.* **1980**, *13*, 419-425.

(4) It must be pointed out in this respect that a diradical may have some ionic character. See ref. 5.

(5) Salem, L.; Rowland, C. *Angew. Chem., Int. Ed. Engl.* **1972**, *11*, 92-111.

0002-7863/90/1512-483$02.50/0

competition between the ene reaction and the formation of dioxetane is possible, polar solvents favor the latter;[6a-f] however, the response is about 3 orders of magnitude lower than expected if polar intermediates were involved.[6g] Both observations could be accommodated either by a radical reaction with substantial polar character,[5,6h] or by an early and relatively nonpolar transition state, possibly leading to a more polar intermediate,[6d] or by a concerted reaction with some charge transfer.[6i,j] The possibility of intervention of diradical intermediates was also considered in some theoretical studies. Harding and Goddard[7] supported the role of CH_2CH_2OO diradicals with extensive calculations at the GVB-CI level with a double-ζ plus polarization basis set. They located the peroxirane minimum higher in energy than the diradical minimum by ca. 8 kcal mol^{-1} and concluded that it is unlikely that peroxiranes play any role in the mechanism of singlet O_2 reactions. Furthermore, the amphoionic structures were estimated to be significantly higher in energy than the peroxy diradical.[7c] Since only intermediate minima (and no saddle points) were studied for the formation of peroxirane and dioxetane, the problem of the pathway actually followed by the system was left open. More recent UHF computations by Yamaguchi et al.,[7d] using both ab initio and MINDO/3 methods, showed that 1,4-diradicals are more stable than perepoxides. However, computations on substituted diradical intermediates suggesting nonstereospecificity and regioselectivity, brought these authors to state that the intermediacy of diradicals is not probable.

Isotope effects[6e,8a] indicate substantial rehybridization[8b] of only one of the two carbon atoms involved in bond formation with oxygen. This seems to rule out both a perepoxide and an early transition state, at least in the cases studied. On the other hand, some authors[8c] find a concerted mechanism of [2s + 2a] character not in contradiction with these results.

The existence of polar intermediates (open-chain zwitterions or perepoxidic structures) has been assumed by some authors in the attempt to rationalize the formation of different cleavage or rearrangement products,[9a] or the formation of solvent-addition products.[9b-d] However, in some of these cases alternative processes are possible (see ref 3a for details). A somewhat polar transition state has been suggested by studies of the temperature dependence of the reactions of $^1\Delta_g$ O_2 with alkenes in methanol[9e] and in the gas phase,[9f] where slightly higher activation energies have been found for the gas-phase reactions.

The formation of epoxides in the reaction of singlet oxygen with a variety of substrates[6j,9a,10a-f] has been interpreted as an evidence

Chart II

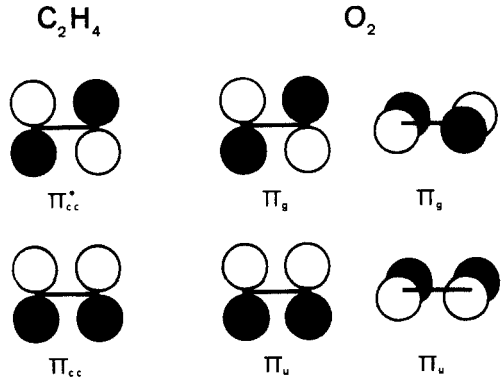

for perepoxidic intermediates[11] followed by abstraction of the terminal oxygen atom possibly by singlet O_2 itself,[10a,i,12c] although free-radical processes have also been proposed.[10j] However, epoxides can arise by other mechanisms,[10g,h] and their formation is affected substantially by radical quenchers. Recent experimental work by Schaap et al., involving an oxygen transfer to sulfoxides and the detection of an epoxide, does not show this effect and claims evidence for the trapping of the elusive perepoxidic intermediate.[10k] The hypothesis of intervention of a perepoxidic intermediate has also been considered in some theoretical studies. In an earlier study Fukui and co-workers[11a] drew attention, on the basis of symmetry considerations, to the possibility that a perepoxidic structure can play a role in the formation of dioxetanes. Inagaki and Fukui,[11b] in a subsequent CNDO/2 study, observed that if perepoxide was an intermediate, its minimum region on the energy hypersurface had to be very shallow and perepoxide would not be isolable, and they suggested for it the term *quasi-intermediate*. Dewar and co-workers[12a-c] concluded, on the basis of earlier MINDO/3 studies on the reaction of O_2 with some substituted alkenes, that these reactions lead initially to intermediate peroxiranes or zwitterions, which subsequently rearrange to the final products. In the case of ethene itself, they found that the reaction proceeds via a polar peroxirane, which in turn rearranges to dioxetane in a rate-determining step. However, the rearrangement to products is more difficult than the back-dissociation to ethene and O_2. More recent MNDO computations put ethene perepoxide 32.6 kcal mol^{-1} above the ethene–dioxygen dissociation limit (in contrast with MINDO/3). However, the perepoxide is still a minimum on the energy surface and is reachable through a perepoxide-like C_s transition state.[12d] The possibility of a charge-transfer mechanism has been investigated in studies of cyclic voltammetry.[13] These studies have shown a correlation between the reduction potentials of some alkenes and their reactivity to give dioxetanes but have not provided conclusive evidence for or against a charge-transfer mechanism.

Various modes of attack with symmetry higher than C_1 were considered by Hotokka, Roos, and Siegbahn[14] in a recent MC-

(6) (a) Bartlett, P. D. *Pure Appl. Chem.* **1971**, *27*, 597–609. (b) Bartlett, P. D.; Schaap, A. P. *J. Am. Chem. Soc.* **1970**, *92*, 3223–3225. (c) Ando, W.; Watanabe, K.; Migita, T. *J. Am. Chem. Soc.* **1974**, *96*, 6766–6768. (d) Bartlett, P. D.; Frimer, A. A. *Heterocycles* **1978**, *11*, 419. (e) Frimer, A. A.; Bartlett, P. D.; Boschung, A. F.; Jewett, J. G. *J. Am. Chem. Soc.* **1977**, *99*, 7977–7986. (f) Bartlett, P. D.; Mendenhall, G. D.; Schaap, A. P. *Ann. N.Y. Acad. Sci.* **1970**, *171*, 79. (g) Williams, J. K.; Wiley, D. W.; McKusick, B. C. *J. Am. Chem. Soc.* **1962**, *84*, 2210–2215. (h) Martin, J. C.; Tuleen, D. L.; Bentrude, W. G. *Tetrahedron Lett.* **1962**, 229–233. (i) Huisgen, R.; Feiler, L. A.; Otto, P. *Tetrahedron Lett.* **1968**, 4485–4490. (j) Huisgen, R.; Feiler, L. A.; Otto, P. *Chem. Ber.* **1969**, *102*, 3444–3459.

(7) (a) Harding, L. B.; Goddard, W. A., III. *J. Am. Chem. Soc.* **1977**, *99*, 4520–4523. (b) Harding, L. B.; Goddard, W. A., III. *Tetrahedron Lett.* **1978**, *8*, 747–750. (c) Harding, L. B.; Goddard, W. A., III. *J. Am. Chem. Soc.* **1980**, *102*, 439–449. (d) Yamaguchi, K.; Yabushita, S.; Fueno, T.; Houk, K. N. *J. Am. Chem. Soc.* **1981**, *103*, 5043–5046.

(8) (a) Frimer, A. A. Ph.D. Thesis, Harvard University, Cambridge, MA, 1974. (b) Halevi, E. A. *Prog. Phys. Org. Chem.* **1963**, *1*, 109, 172. (c) Alder, R. W.; Baker, R.; Brown, J. M. In *Mechanisms in Organic Chemistry*; Wiley: New York, 1971; p 260.

(9) (a) Takeshita, H.; Hatsui, T.; Jinnai, O. *Chem. Lett.* **1976**, 1059. (b) Fenical, W.; Kearns, D. R.; Radlick, P. *J. Am. Chem. Soc.* **1969**, *91*, 3396–3398. (c) Foote, C. S.; Mazur, S.; Burns, P. A.; Lerdal, D. *J. Am. Chem. Soc.* **1973**, *95*, 586–588. (d) Easton, N. R.; Anet, F. A. L.; Burns, P. A.; Foote, C. S. *J. Am. Chem. Soc.* **1974**, *96*, 3945–3948, 4339–4340. (e) Koch, E. *Tetrahedron* **1968**, *24*, 6295–6318. (f) Ashford, R. D.; Ogryzlo, E. A. *J. Am. Chem. Soc.* **1975**, *97*, 3604–3607.

(10) (a) Bartlett, P. D. *Chem. Soc. Rev.* **1976**, *5*, 149–163. (b) Adam, W. *Adv. Heterocycl. Chem.* **1977**, *21*, 437–481. (c) Schaap, A. P.; Faler, G. R. *J. Am. Chem. Soc.* **1973**, *95*, 3381–3382. (d) Yang, N. C.; Carr, R. V. *Tetrahedron Lett.* **1972**, 5143–5145. (e) Jefford, C. W.; Boschung, A. F. *Helv. Chim. Acta* **1974**, *57*, 2242–2261. (f) McCapra, F.; Behesti, I. *J. Chem. Soc., Chem. Commun.* **1977**, 517–518. (g) Jefford, C. W.; Boschung, A. F. *Chimia* **1977**, *31*, 60. (h) Bartlett, P. D.; Landis, M. E. *J. Am. Chem. Soc.* **1977**, *99*, 3033–3037. (i) Vernin, G.; Trappendhal, S.; Metzger, J. *Helv. Chim. Acta* **1977**, *60*, 284–297. (j) Jefford, C. W.; Boschung, A. F. *Ibid.* 2673–2685. (k) Schaap, A. P.; Recher, S. G.; Faler, G. R.; Villasenor, S. R. *J. Am. Chem. Soc.* **1983**, *105*, 1691–1693.

(11) (a) Inagaki, S.; Yamabe, S.; Fujimoto, H.; Fukui, K. *Bull. Chem. Soc. Jpn.* **1972**, *45*, 3510–3514. (b) Inagaki, S.; Fukui, K. *J. Am. Chem. Soc.* **1973**, *97*, 7480–7484.

(12) (a) Dewar, M. J. S. *Chem. Br.* **1975**, *11*, 97–106. (b) Dewar, M. J. S.; Thiel, W. *J. Am. Chem. Soc.* **1975**, *97*, 3978–3986. (c) Dewar, M. J. S.; Griffin, A. C.; Thiel, W.; Turchi, I. J. *Ibid.* 4439–4440. (d) Thiel, W. Private communication.

(13) Eriksen, J.; Foote, C. S.; Parker, T. L. *J. Am. Chem. Soc.* **1977**, *99*, 6455–6456.

(14) Hotokka, M.; Roos, B.; Siegbahn, P. J. *J. Am. Chem. Soc.* **1983**, *105*, 5263–5269.

SCF and CCI study. They found that the formation of the peroxirane intermediate is easier than passing through a C_s syn-diradical pathway. Although the level of their calculation is good (eight active orbitals in the MC-SCF valence space and basis sets of double-ζ and double-ζ plus polarization quality), some doubt still remains about the reaction paths. Because of symmetry and geometry constraints consistently used in the optimizations, it is not clear whether the structures reported represented true transition structures or higher order saddle points.

The wide spectrum of possibilities appearing in the various experimental and theoretical papers brought Frimer to conclude in 1979[3a] that no definite conclusions could yet be drawn and that the mechanism had still to be made clear. Although since then additional experimental[3d,e,10k] and theoretical[7c,d,14,15b] work has appeared, his statement still seems to be valid.

On the theoretical side, a full optimization and unambiguous characterization of the various intermediates and transition structures are desirable to provide a more reliable assessment of the different pathways. The present study[15] has been undertaken with the aim of providing a reliable qualitative description of the potential energy hypersurface of the model system $O_2 + C_2H_4$. Therefore, several modes of attack are analyzed to determine whether they lead to true transition structures, and hence to pathways of chemical interest, or to higher order saddle points of no chemical relevance. This requires full optimization of the geometries of the critical points and their characterization by computing the curvature of the energy surface at each of them.

Method

Calculations were carried out at the MC-SCF level of theory, with standard minimal (STO-3G)[16a] and split-valence shell (4-31G)[16b] basis sets. The MC-SCF and CI codes[17] are used in conjunction with the GAUSSIAN82 series of programs.[18] The valence space used in the present MC-SCF computations consists of six active orbitals that are more directly involved in bond formation and breaking. For the separate reactants these are the π and π^* orbitals of ethene and the two degenerate pairs of O_2, π_g, and π_u (Chart II).

With this choice, diradical species are described in the same manner as closed-shell species and proper dissociation of both into the two original subsystems is guaranteed. In the computations on the peroxirane minimum and related saddle point, it appeared desirable to include in the active space the highest occupied σ and the lowest unoccupied σ^* orbitals of O_2. At the same time, 4-31G computations on these structures carried out with six valence orbitals showed a slow convergence rate, due to the inclusion in the active space of a doubly occupied orbital (population greater than 1.99 electrons) localized on the terminal oxygen. For these reasons the C_s approach leading to peroxirane was studied with the 4-31G basis set in a space of seven active orbitals, having included the σ and σ^* of O_2 and excluded one terminal oxygen lone pair. Although it would have been desirable to introduce additional active orbitals (as the σ and σ^* couple for O_2) in all the computations to achieve a better description of the electron distribution changes that occur during the reaction, this "minimal" choice has been dictated by the extensive geometry optimizations undertaken. A complete CI (105 configuration functions for six valence orbitals and 490 configuration functions for seven valence orbitals) was performed in the valence space, providing size-consistent energies.

The geometries of the critical points have been completely optimized with both basis sets by gradient methods;[19a-d] then, by computing the number of negative eigenvalues (index) of the second-derivative (Hessian) matrix,[19e] these critical points have been characterized as minima (index 0) or saddle points (index 1 for transition structures or >1 for higher order saddle points of no chemical interest). The Hessian has been calculated numerically (with the same basis set used to determine the geometries) in the subspace of the internal coordinates of the non-hydrogen atoms. The Hessian matrix of the saddle points (where the internal coordinates of the hydrogen atoms might be more significantly coupled with the other degrees of freedom) have been recomputed analytically[20] at the STO-3G level with the appropriate critical point geometries. Only these better quality results are discussed, when available.

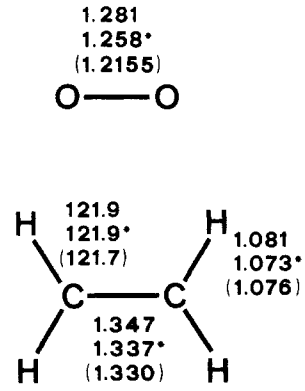

Figure 1. Optimized geometrical parameters of the oxygen molecule ($^1\Delta_g$ state) and ethene. STO-3G values and 4-31G values (starred) are given with experimental values in parentheses. Units: bond lengths, angstroms; angles, degrees.

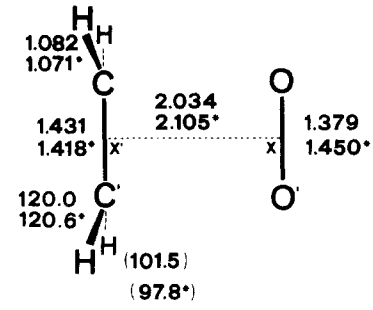

Figure 2. Optimized geometrical parameters of the C_{2v} supra-supra third-order saddle point. STO-3G values and 4-31G values (starred) are given. Units: bond lengths, angstroms; angles, degrees; hydrogen dihedral angles (HCC/CCO) (in parentheses), degrees.

Results and Discussion

The presence of two low-energy adiabatic surfaces, intersecting at some geometries, characterizes the description of the evolution of the $O_2 + C_2H_4$ system. At infinite separation the lowest electronic states are two degenerate singlets, originating from a coupling of the $^1\Delta_g$ states of O_2 with the ground state of ethene. At closer distances (e.g., at those distances at which saddle points are found on the lower energy hypersurface) the following features of the two lowest singlet states can be noticed: (i) these states are no longer degenerate but still rather close in energy; (ii) they have mixed-in contributions from other singlets of the appropriate symmetry, which at infinite separation are located at a relatively high energy; (iii) they are associated with two surfaces that describe different stable species and that are of different symmetry in the presence of a molecular symmetry plane. One of these surfaces is related to the singlet ground state of the product, dioxetane, and is stabilized by a geometrical situation close to that. The other surface is related to the singlet ground state of a planar peroxy diradical and is found to be the lowest surface in correspondence with geometries close to that of this species. To clarify

(15) (a) Preliminary results obtained with the minimal basis set on some selected modes of attack were presented at the international conference TOR85 (Theory of Organic Reactions) held in Gargnano, Italy, June 1985. (b) Tonachini, G.; Schlegel, H. B.; Bernardi, F.; Robb, M. A. *Theochem* **1986**, *138*, 221-227.

(16) (a) Hehre, W. J.; Stewart, R. F.; Pople, J. A. *J. Chem. Phys.* **1969**, *51*, 2657-2664. (b) Ditchfield, R.; Hehre, W. J.; Pople, J. A. *J. Chem. Phys.* **1971**, *54*, 724-728.

(17) Robb, M. A.; Eade, R. H. A. *NATO Adv. Study Inst. Ser., Ser. C* **1981**, *67*, 21-54. Hegarty, D.; Robb, M. A. *Mol. Phys.* **1979**, *38*, 1795-1812.

(18) Binkley, J. S.; Whiteside, R. A.; Krishnan, R.; Seeger, R.; DeFrees, D. J.; Schlegel, H. B.; Topiol, S.; Kahn, L. R.; Pople, J. A. *QCPE* **1981**, *13*, No. 406.

(19) (a) Schlegel, H. B. In *Computational Theoretical Organic Chemistry*; Csizmadia, I. G., Daudel, R., Eds.; D. Reidel: Dordrecht, The Netherlands, 1981; pp 129-159. (b) Schlegel, H. B. *J. Chem. Phys.* **1982**, *77*, 3676-3681. (c) Schlegel, H. B.; Binkley, J. S.; Pople, J. A. *J. Chem. Phys.* **1984**, *80*, 1976-1981. (d) Schlegel, H. B. *J. Comput. Chem.* **1982**, *3*, 214-218. (e) Mezey, P. G. Potential Energy Hypersurfaces. *Studies in Physical and Theoretical Chemistry*; Elsevier: New York, 1987; Vol. 53.

(20) In the case of the supra-antara critical point in the ethene dimerization reaction, the analytical Hessian calculation produced a result in contrast with the previous numerical calculations of selected Hessian rows, which was limited to the internal coordinates of non-hydrogen atoms. This result stresses the importance of including bending and torsions relevant to the CH_2 groups in heavily distorted geometries.

Table I. Total[a] and Relative[b] Energies of the Critical Points

	STO-3G		4-31G[c]	
	E	ΔE	*E*	ΔE
dissociation limit	−224.774 311	0.0	−227.344 609	0.0
supra–supra (3rd-order saddle pt)	−224.690 755	52.5	−227.262 535	51.5
supra–antara (2nd-order saddle pt)	−224.691 941	51.7	−227.264 700	50.1
syn-diradicaloid Π3 (2nd-order saddle pt)	−224.726 466	30.0	−227.291 778	33.2
syn-diradicaloid Π4 (2nd-order saddle pt)	−224.711 347	39.5		
gauche-diradicaloid (1st-order saddle pt)	−224.728 454	28.8	−227.297 524	29.5
anti-diradicaloid (1st-order saddle pt)	−224.726 775	29.8	−227.293 022	32.4
syn-diradical (min)	−224.742 945	19.7		
gauche-diradical (min)	−224.746 082	17.7	−227.308 287	22.8
anti-diradical (min)	−224.745 400	18.1	−227.307 383	23.4
peroxirane (min)	−224.694 670	50.0	*−227.370 479*	*(0.0)*
peroxirane-like (2nd-order saddle pt)	−224.673 727	63.1	*−227.348 773*	*(13.6)*
dioxetane (min)	−224.812 771	−24.1	−227.350 900	−4.0

[a] Hartrees. [b] Kilocalories per mole. [c] Italicized entries correspond to computations performed with an active space of seven orbitals (see text). ΔE: peroxirane-like saddle point with respect to peroxirane minimum.

the relationships between the two surfaces corresponding to the lowest singlets, the features of the critical points found for each geometrical approach on the lowest surface will be now discussed. Then the relationships between some pairs of critical points will be examined, and in one case, they will be discussed in relation to a critical point belonging to the upper singlet surface.

Total energies for the minima and saddle points discussed in this paper are reported in Table I together with the energy differences relative to the $C_2H_4 + O_2$ dissociation limit. The relevant optimized structures are reported in Figures 1–4 and 6–12. The different modes of attack and their symmetry have been outlined in Chart I and will be discussed in the following.[21] The optimum geometrical parameters obtained for O_2 and C_2H_4 are shown in Figure 1.[24]

(1) C_{2v} Supra–Supra Concerted Approach. Search for a saddle point within C_{2v} symmetry (that of dioxetane) leads to the optimized geometry shown in Figure 2. The analytical Hessian matrix computed at this point shows three negative eigenvalues (i.e., the structure corresponding to this critical point is characterized by three imaginary vibrational frequencies): the first one corresponds to an eigenvector dominated by *R*, the distance between the midpoints of the CC and OO bands (denoted by X′ and X, respectively, in Figure 2); the second (smaller) negative eigenvalue is related to the torsional angle along the C_2 axis (Φ); the third negative eigenvalue is related to a deformation along a combination (with the same sign) of two planar angles (CX′X and X′XO). This critical point is therefore classified as a third-order saddle point and is of no chemical interest. The critical point just discussed lies on the energy hypersurface corresponding to the lowest singlet. This state is described in terms of configurations that can be classified as symmetric (S) with respect to a reflection through the molecular plane: the resulting wave function shows an approximate double occupancy of the two molecular orbitals localized on the two oxygen atoms and perpendicular to the molecular plane. This singlet electronic state

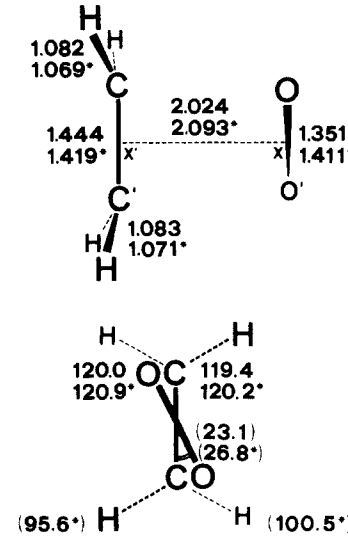

Figure 3. Optimized geometrical parameters of the C_2 supra–antara second-order saddle point. STO-3G values and 4-31G values (starred) are given. Units: bond lengths, angstroms; angles, degrees; hydrogen dihedral angles (HCC/CX′X) (in parentheses), degrees.

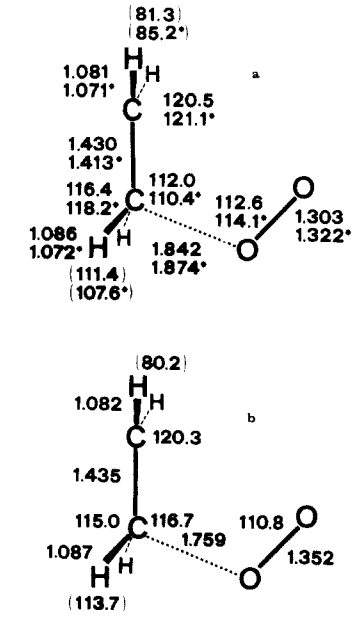

Figure 4. (a) Optimized geometrical parameters of the C_s syn second-order saddle point on the Π3 surface. STO-3G values and 4-31G values (starred) are given. (b) Optimized geometrical parameters of the C_s syn second-order saddle point on the Π4 surface. STO-3G values only are given. Units: bond lengths, angstroms; angles, degrees; hydrogen dihedral angles (HCC/CCO) (in parentheses), degrees.

(21) It could be desirable to classify some modes of approach of O_2 and ethene in terms of *symmetry-allowed* and *symmetry-forbidden* pathways,[22] in analogy to what is usually done for the ethene dimerization reaction (for instance, the supra–supra and supra–antara approaches of dioxygen and ethene were classified[2a,23] as symmetry-forbidden and symmetry-allowed, respectively). However, Harding and Goddard warned that the diradical character of the doubly degenerate $^1\Delta_g$ state of O_2 can invalidate this kind of analysis in some cases.[2b,13c] Orbital and state correlation diagrams[22] could be drawn[23] only if in an early stage of the reaction there is resolution of the degeneracy, if the diradical character of O_2 disappears and the oxygen molecule can be described mainly with a single configuration made up by doubly occupied orbitals.

(22) (a) Woodward, R. B.; Hoffmann, R. *The Conservation of Orbital Symmetry*; Verlag Chemie and Academic Press: Weinheim and New York, 1970. (b) Longuet-Higgins, H. C.; Abrahamson, E. W. *J. Am. Chem. Soc.* **1965**, *87*, 2045–2046 (c) Hoffmann, R.; Woodward, R. B. *Ibid.* 2046–2048. (d) Hoffmann, R. *Trans. N.Y. Acad. Sci.* **1968**, *28*, 475. (e) Hoffmann, R.; Woodward, R. B. *Acc. Chem. Res.* **1968**, *1*, 17.

(23) Kearns, D. R. *J. Am. Chem. Soc.* **1969**, *91*, 6554–6563.

(24) From Figure 1 it can be seen that the OO bond length is longer than experiment[25a] by 0.042 Å with the 4-31G basis set; the geometrical parameters of ethene agree well with experiment.[25b]

(25) (a) Herzberg, G. *Diatomic Molecules*, 2nd ed.; Van Nostrand: Princeton, NJ, 1950. (b) Callomon, J. H.; Hirota, E.; Kuchitsu, K.; Lafferty, W. J.; Maki, A. G.; Pote, C. S. Structure Data on Free Polyatomic Molecules. *Numerical Data and Function Relationships in Science and Technology*; Landolt-Bornstein New Series; Hellwege, K. H., Ed., Springer-Verlag: West Berlin, 1976; Vol. 7.

and the related energy hypersurface could then be labeled as Π4.

(2) C_2 Supra–Antara Concerted Approach. The instability of the C_{2v} supra–supra critical point with respect to a torsion around the C_2 axis suggests the existence of a C_2 critical point related to it by this geometrical deformation. This geometry would permit both of the π_g orbitals of the oxygen molecule to interact with the π system of ethene. An approach of this kind (supra for C_2H_4 and antara for O_2) was suggested by Bartlett.[10a] Optimization leads to a structure with a rather small value of the torsional angle, Φ (Figure 3); its energy is ca. 1 kcal mol^{-1} lower than that of the C_{2v} critical point (see Table I). Despite the fact that it is a minimum with respect to Φ, this critical point is a second-order saddle point, again of no chemical interest. One of the two directions of negative curvature is dominated by R, the second one by a "trapezoidal" distortion similar to that encountered in the supra–supra critical point, corresponding to a combination with the same sign of the CX′X and X′XO planar angles. Relaxation of the geometry along this degree of freedom would lead to a C_1 (gauche) geometry, which would correspond to a structure with some diradicaloid character.

(3) C_s Syn-Diradicaloid Approach. The aforementioned in-plane distortion of the C_{2v} supra–supra critical point, related to a direction of negative curvature of the energy hypersurface, points to a C_s syn structure where the CCOO molecular symmetry plane is still present but the CC and OO bonds are no longer parallel. Optimization of this geometry for the lowest singlet wave function leads to a critical point corresponding to a structure (Figure 4a) endowed with some diradicaloid character. If this syn critical point were a transition structure (and in the absence of a diradical minimum with syn geometry directly related to it), the reaction would be a one-step (concerted) one, with asynchronous bond formation. Again this structure is found to be a second-order saddle point, where the first direction of negative curvature is dominated by the shorter CO distance and the second one by the CCOO torsional angle: a deformation along this torsional angle would lead through a very flat region of the energy hypersurface to a C_1 gauche geometrical structure. Thus, the nature of this critical point does not allow the existence of a minimum energy diradical pathway passing through a structure of this kind.

Although the search for a critical point with syn geometry might have been suggested by the third direction of negative curvature found in the C_{2v} saddle point, it must be pointed out that there is no direct relationship between this syn structure and the supra–supra structure because they belong to two different electronic state surface. For the syn structure the lowest singlet wave function corresponds to a Π3 state, antisymmetric (A) with respect to reflection through the molecular plane and characterized by a dominant contribution of configurations where the π molecular orbitals perpendicular to the molecular plane (and significantly localized on the two oxygen atoms) have an occupancy of three electrons. The symmetry plane coincident with the molecular plane is kept on going from the C_{2v} structure to the C_s structure, and the different symmetries of the two electronic states involved (Π3, A; Π4, S) indicate the presence of a real crossing of surfaces. Thus, the C_{2v} supra–supra critical point cannot be directly related to the syn critical point found on the lowest singlet surface; on the other hand it might be directly related, by the same in-plane (CC′O′ + C′O′O) angle opening deformation, to a structure lying on the next singlet (Π4) surface (which is located approximately 9 kcal mol^{-1} above the lowest singlet surface at the syn geometry). The structure shown in Figure 4b belongs to a Π4 syn saddle point: it has been determined and characterized (at the STO-3G level only) with the aim of assessing the possibility of the presence of a syn transition structure on the upper surface. But this syn structure is again a second-order saddle point:[26] although the orbital occupancy is different from the Π3 saddle point, and at first sight more favorable to ring closure, this structure is unstable with respect to a torsion along the CCOO dihedral angle, as well as a shortening of the CO distance. The relationship between the

(26) For this reason the study of this structure has not been pursued at the 4-31G level.

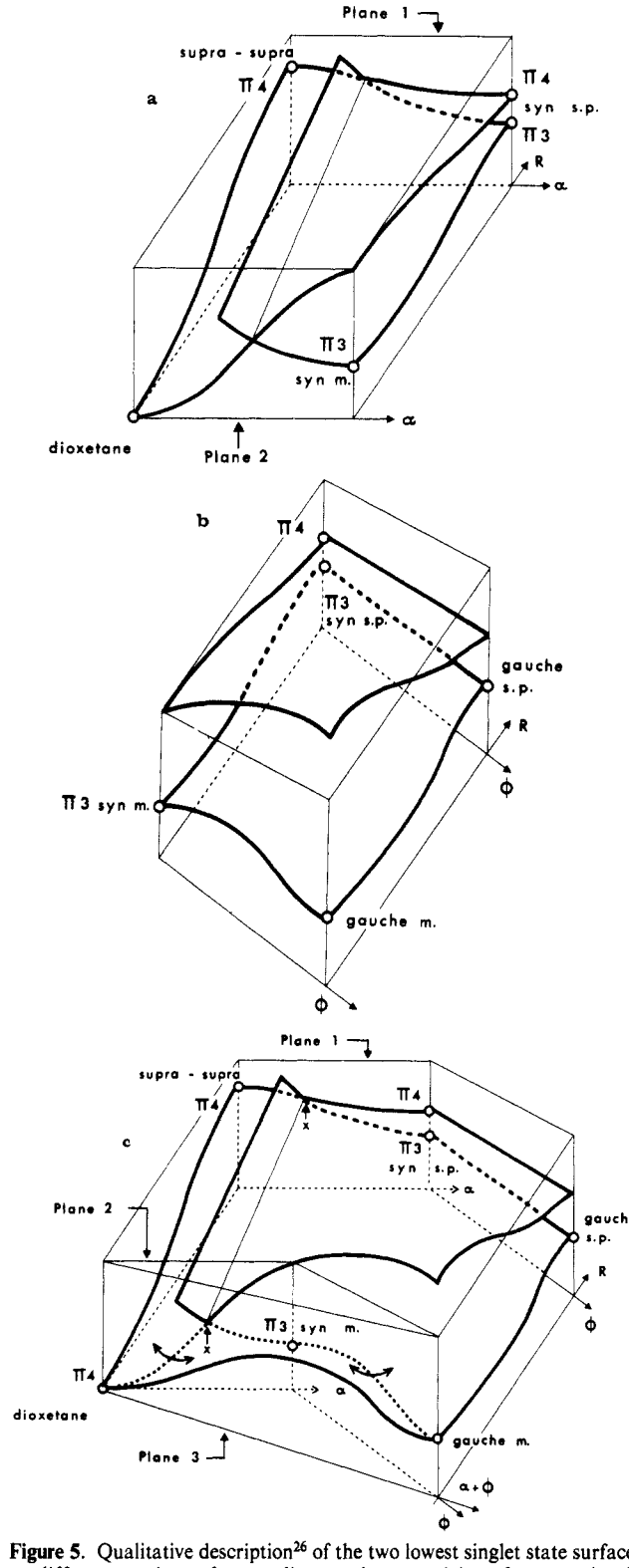

Figure 5. Qualitative description[26] of the two lowest singlet state surfaces on different sections of a coordinate subspace: (a) surface crossing in connection with geometrical deformations leading from the supra–supra to the syn saddle point or from the syn-diradical to dioxetane (section along α); (b) two lowest energy surfaces for the syn- and gauche-diradicaloid saddle points and diradical minima (section along Φ); (c) surfaces in Figure a and b are merged with a portion of the lowest singlet surface, connecting the gauche minimum to dioxetane (section along α + Φ) to stress that a single surface is present, folded on itself. Plane 1: real crossing (X) corresponding to the opening of the CCO and COO angles (denoted by α) leading from the supra–supra saddle point to the syn saddle point. Plane 2: real crossing (X) corresponding to the path syn saddle point–syn-diradical minimum–dioxetane. Plane 3: avoided crossing corresponding to the closure of the gauche-diradical minimum to dioxetane; only the lower surface shown. (For every path more states than shown mix together.)

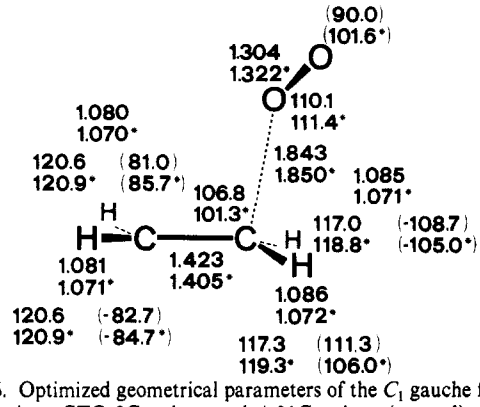

Figure 6. Optimized geometrical parameters of the C_1 gauche first-order saddle point. STO-3G values and 4-31G values (starred) are given. Units: bond lengths, angstroms; angles, degrees; dihedral angles (HCC/CCO and OOC/OCC) (in parentheses), degrees.

two surfaces and the corresponding critical points in function of the in-plane opening (CC'O' + C'O'O) is shown in Figure 5a, plane 1 (C_s symmetry maintained).[27]

As Harding and Goddard pointed out in discussing the electronic structure of the peroxy diradical,[7c] the syn geometry should not be favorable to direct closure to dioxetane, due to the occupancy of the p orbitals in the diradical. This is basically true also for the Π3 saddle-point structure discussed above: here a rotation along the forming CO bond seems to ease a three-electron repulsion present in the planar syn structure. Both these qualitative considerations and the second direction of negative curvature found in the Π3 syn critical point suggest that a minimum energy pathway is to be looked for within C_1 symmetry, i.e., in correspondence to a gauche approach. This was already indicated by a preliminary numerical Hessian computation with the minimal basis set.[15b]

(4) C_1 Gauche Diradicaloid Transition Structure. For the C_1 mode of approach, a first-order saddle point is found (Figure 6), at ca. 29 kcal mol^{-1} above the dissociation limit (see Table I). The eigenvector corresponding to the single negative eigenvalue of the Hessian is dominated by the shorter CO distance. By comparison of Figure 6 with Figures 2–4, it can be seen that this transition structure occurs at a distance between the two reacting species that is shorter than that encountered in the higher order saddle points corresponding to the concerted synchronous modes of attack (supra–supra and supra–antara), but which is very close to that found in the syn second-order saddle point. The opening of the torsional angle that leads from the syn to the gauche transition structure is more pronounced in the geometry optimized with the extended basis (102°) than with the minimal basis (90°); the distance between the two reacting molecules (the shorter CO distance) does not show a similar basis set dependence. If this transition structure were to lead directly to dioxetane, the reaction would appear to be "one-step" and concerted, although highly asynchronous. If on the contrary a gauche diradical existed as a well-defined minimum on the energy hypersurface, the reaction would require two steps to form dioxetane and would therefore be nonconcerted.

(5) Anti Transition Structure. Closely related to the gauche-diradical pathway is an antiperiplanar approach. The anti structure is a first-order saddle point located 30–32 kcal mol^{-1} above the dissociation limit (see Table I). Its geometry (Figure 7) is very similar to the gauche transition structure. The direction of negative curvature is described by an eigenvector dominated by the shorter CO distance. The structure is stable with respect

(27) The plotted energies have been obtained by MC-SCF orbital optimizations for the lowest singlet at a given geometry. The geometries were generated by linearly interpolating the geometrical parameters between the two critical points considered (see Figure 5): between the supra–supra and syn saddle points, plane 1; between the syn minimum and dioxetane, plane 2; between the gauche saddle point and dioxetane, plane 3. The avoided crossing shown between the gauche minimum and dioxetane is generated from the interaction with other singlet surfaces (not shown for clarity) located at a relatively high energy at infinite separation.

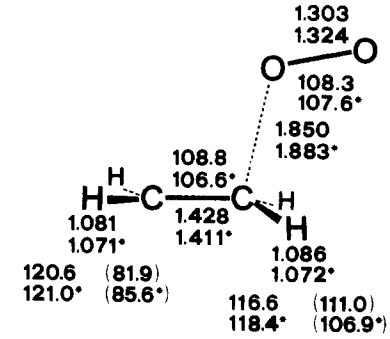

Figure 7. Optimized geometrical parameters of the C_s anti first-order saddle point. STO-3G values and 4-31G values (starred) are given. Units: bond lengths, angstroms; angles, degrees; hydrogen dihedral angles (HCC/CCO) (in parentheses), degrees.

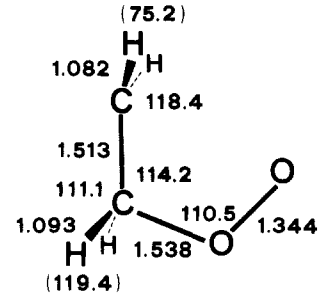

Figure 8. Optimized geometrical parameters of the C_s syn-diradical minimum. STO-3G values only are given. Units: bond lengths, angstroms; angles, degrees; hydrogen dihedral angles (HCC/CCO) (in parentheses), degrees.

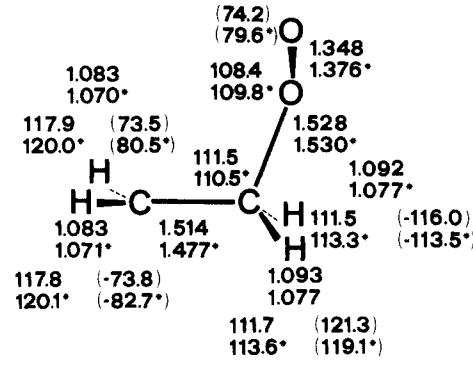

Figure 9. Optimized geometrical parameters of the C_1 gauche-diradical minimum. STO-3G values and 4-31G values (starred) are given. Units: bond lengths, angstroms; angles, degrees; dihedral angles (HCC/CCO and OOC/OCC) (in parentheses), degrees.

to a rotation along the CCOO dihedral angle, connecting it to the gauche transition structure. The same considerations about the Π3 and Π4 states developed for the syn saddle point apply to the anti transition structure, where the CCOO molecular plane is a symmetry plane just as in the syn. The features of the anti transition structure suggest the existence of a minimum with the same kind of geometry.

(6) Diradical Minima. The diradical path corresponds to a two-step reaction, because the peroxy diradical is a stable species. Indeed, three conformational minima are present on the surface, corresponding to the syn, the gauche, and the anti approaches discussed above. Therefore, the possibility of a concerted pathway having diradical character can be ruled out. (i) A syn minimum (Figure 8) exists on the surface, although not reachable directly through an approach of the same symmetry (the syn saddle point of Figure 4 was found to be a second-order saddle point). Contrary to the syn saddle point, which was unstable with respect to a rotation leading to the gauche saddle point, the syn minimum presents a tiny barrier in that direction. This structure cannot be put in direct relation with dioxetane through a C_s reaction path[26] (see below). (ii) A second minimum (related to the transition

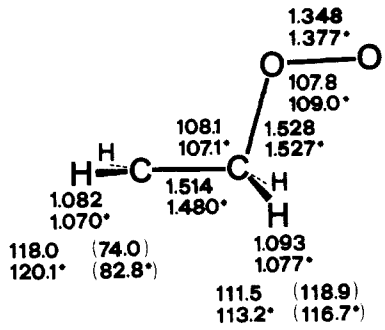

Figure 10. Optimized geometrical parameters of the C_s anti-diradical minimum. STO-3G values and 4-31G values (starred) are given. Units: bond lengths, angstroms; angles, degrees; hydrogen dihedral angles (HCC/CCO) (in parentheses), degrees.

structure of Figure 6) is found corresponding to a gauche-diradical structure (Figure 9). It can be noted in passing that the CCOO dihedral angle value (74–80°) is considerably smaller than in the transition structure. As seen from Table I, this minimum is located at about 18–23 kcal mol^{-1} above the dissociation limit (depending on the basis set) and has a sizable barrier to redissociation (7–11 kcal mol^{-1}). It is more stable than the syn minimum by ca. 2 kcal mol^{-1}. (iii) A minimum is found also corresponding to the anti transition structure of Figure 7. It is located ca. 0.5 kcal mol^{-1} higher in energy than the gauche minimum, and its geometrical parameters (Figure 10) are very close to those of the gauche minimum.

The lowest singlet corresponds for both the syn and the anti minima to a Π3 state (A). Direct closure of the syn diradical to dioxetane, whose lowest singlet is Π4 (S), is prevented by the existence of a real crossing between these two surfaces of different symmetry along a direction connecting the two minima. The surface crossing is shown in Figure 5a, plane 2 (C_s symmetry maintained).[27] This situation is obviously very similar to that encountered when discussing the relationship between the supra–supra and syn saddle points (Figure 5a, plane 1). Dioxetane can, on the contrary, be reached along a C_1 gauche path because the two singlet functions can in that case mix: the surfaces would then "repel" each other, and the system could evolve through this avoided crossing from the diradical minimum to dioxetane (Figure 5c, plane 3). The gauche diradical is therefore an intermediate (possibly short-lived) in this reaction. Further investigation would be required to determine the height of the barrier for the closure to dioxetane.[28] A low barrier and very short lifetime would be consistent with the experimental evidence that radical traps are ineffective in quenching singlet O_2 reactions.

(7) Peroxirane Minimum. A perepoxidic intermediate has been often invoked[10c,f,k] as a possible rationalization of experimental findings. In the present study peroxirane has been found to correspond to a minimum on the energy hypersurface. Its geometrical structure is shown in Figure 11a. Unfortunately, the energy of this critical point is rather basis set dependent, as can be seen from Table I: yet, the main objective at this point is not to assess the energy difference between the peroxirane minimum and the gauche-diradical minimum but to determine whether this minimum can be reached through a pathway independent from the diradical pathway described above.

(8) The C_s Peroxirane-like Attack. The next step has been, therefore, the search for a saddle point with the same symmetry as the peroxirane minimum. An approach with C_s symmetry leads to the structure shown in Figure 11b. This critical point does not correspond to a transition structure, being unstable not only with respect to a deformation described mostly by R (the distance between the midpoint X of the CC bond and the closest oxygen atom, O′) but also with respect to an opening of the CXO′ planar

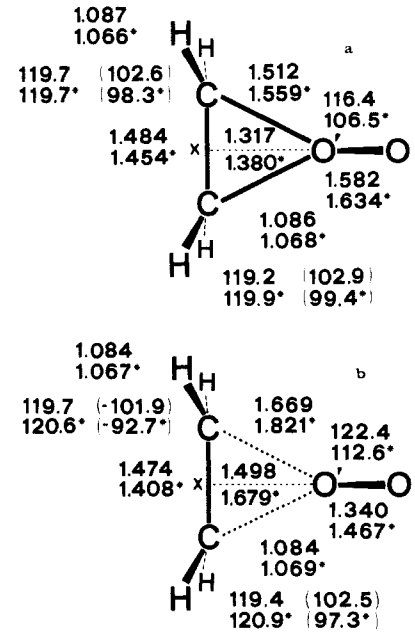

Figure 11. (a) Optimized geometrical parameters of the C_s peroxirane minimum. (b) Optimized geometrical parameters of the C_s peroxirane-like second-order saddle point. STO-3G values and 4-31G values (starred) obtained by an active space of seven orbitals (see text). Units: bond lengths, angstroms; angles, degrees; hydrogen dihedral angles (HCC/CCO′) (in parentheses), degrees.

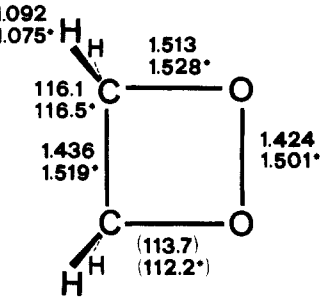

Figure 12. Optimized geometrical parameters of the C_{2v} dioxetane minimum. STO-3G values and 4-31G values (starred) are given. Units: bond lengths, angstroms; angles, degrees; hydrogen dihedral angles (HCC/CCO) (in parentheses), degrees.

angle, pointing toward the C_1 diradicaloid transition structure. These results confirm the minimal basis set findings of the preliminary study.[15b] The system cannot, therefore, evolve from O_2 and C_2H_4 at infinite separation to the peroxirane minimum following a path with the same symmetry as peroxirane. The only viable path to peroxirane seems to be through the gauche-diradical minimum.[28]

(9) Dioxetane Minimum. The optimized geometrical parameters of the reaction product, dioxetane, are reported in Figure 12. The energy difference with respect to the dissociation limit shows a basis set dependance similar to that found for the peroxirane minimum. A comparison of the computed geometry with the available experimental structural data[29] is complicated by the presence of different substituents that give rise to significant variations in bond lengths and angles.

For deformations that maintain a plane of symmetry in the molecule, the two surfaces described above can undergo real crossings.[30] These deformations connect two geometrical situations corresponding to (a) an in-plane approach leading to di-

(28) The determination of the height of the barrier separating the gauche minimum from the two cyclic minima, as well as a comparison with the barrier separating peroxirane from dioxetane, would require further investigation at a higher computational level.

(29) See for instance: (a) Krebs, A.; Schmalstieg, H.; Jarchow, O.; Klaska, K. H. *Tetrahedron Lett.* **1980**, *21*, 3171–3174. (b) Adam, W.; Arias, L. A.; Zahn, A.; Zinner, K.; Peters, K.; Peters, E. M.; von Schnering, H. G. *Ibid.* **1982**, *23*, 3251–3254. (c) Adam, W.; Cilento, G. *Angew. Chem., Int. Ed. Engl.* **1983**, 529–542.

(30) Salem, L.; Leforestier, C.; Segal, G.; Wetmore, R. *J. Am. Chem. Soc.* **1975**, *97*, 479–487.

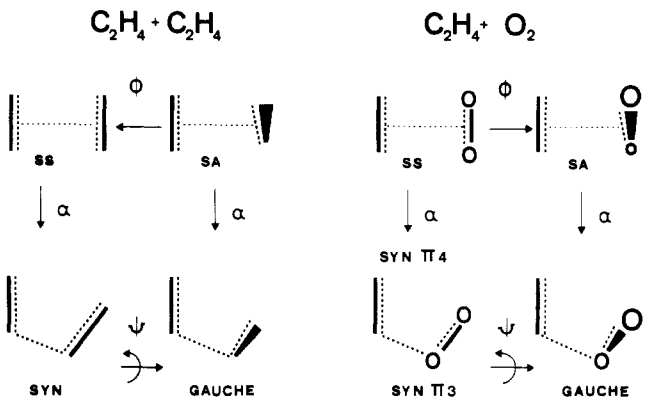

Figure 13. Schematic comparison of the nature of the saddle points shared by the ethene + ethene system and by the oxygen molecule + ethene system. Arrows departing from a critical point indicate the directions of negative curvature. Direction of negative curvature dominated by the distance between the two moieties is shared by all the critical points and is not shown.

oxetane and (b) an approach corresponding to a planar peroxy diradical. As a consequence, the saddle points found on the lowest energy surface for different geometrical approaches can correspond to one or the other of these two electronic states. The energy barriers found as the two moieties approach these saddle points are generated by avoided crossings[30] with different higher energy surfaces, depending on the geometrical approach, a or b, which are related to electronic states of the appropriate symmetry. On the other hand, deformations destroying the molecular plane of symmetry can relate saddle points (as well as minima) of types a and b through a motion on the same (lower) surface. This latter possibility shows that the point representative of the system can be moved from one surface to the other without discontinuity, for example from the Π3 syn saddle point through the gauche saddle point and minimum to dioxetane, to the supra–supra saddle point, and finally to the Π4 syn saddle point. In other words, the surface shown in Figure 5 is actually only one, folded on itself. At closer distances, where minima on the lowest singlet energy hypersurface have been found, the splitting between the ground state and the next singlet becomes much larger, but again the two singlets can go through a reversal of the energetic ordering. When this happens, a real crossing or an avoided crossing can again occur depending on the symmetry of the system.[30] These features have been described in Figure 5 for three selected modes of attack (planes 1–3).[27]

The evolution from reactants to products of the O_2 + ethene reaction presents some analogies with the previously studied[31] ethene + ethene reaction. Yet the evolution of the latter system in its ground state is described by a single adiabatic surface: therefore, the comparison of geometrically similar structures in the two chemical systems is appropriate only if the bonding situation, i.e., the electronic spin coupling, found for the $O_2 + C_2H_4$ surface critical point is the same as the corresponding ethene + ethene surface critical point. In the presence of the appropriate molecular symmetry, this happens on the Π4 surface: dioxetane has a counterpart in cyclobutane, and the same is true for the two supra–supra saddle points; the tetramethylene diradical-like syn and anti saddle points are comparable with the Π4 critical points of similar geometry lying on the "upper surface" discussed above. When the symmetry is lowered, as in the gauche approach, the critical points in the two systems are in the same electronic spin-coupling situation. Some similarities and differences in the qualitative features of the energy hypersurfaces pertaining to the two systems will be briefly examined in the following, discussing the nature of the critical points, i.e., the negative eigenvalues and corresponding eigenvectors found in the relevant Hessian computations.[20] The relationships between the critical points in the two systems are schematically shown in Figure 13. The supra–supra, the supra–antara, and the closely related syn-diradicaloid approach are shared by both systems. The nature of the supra–supra critical point is different for the two systems. For both the O_2 + ethene and the ethene + ethene systems the first direction of negative curvature is dominated by a coordinate expressing the distance R between the two interacting molecules, coupled mainly with the CC and OO (or CC) stretchings. The second direction of negative curvature is associated with an in-plane opening/closure motion expressed by the CX′X and OXX′ (or CXX′) angles (denoted by α in Figure 13). The O_2 + ethene system presents a third negative eigenvalue of the Hessian, associated to a rotation around the C_2 axis (this torsional angle is denoted as Φ in Figure 13); for the ethene + ethene system this torsion is associated with a positive Hessian eigenvalue. As it is shown in Figure 13, the α in-plane opening approximately points toward the syn saddle point, while the Φ torsion leads to the supra–antara saddle point. The nature of the supra–antara[31d] and the syn critical points is the same for both systems: they show two directions of negative curvature and are classified as second-order saddle points. In the syn saddle point the first direction of negative curvature of the surface is dominated for both systems by a coordinate expressing the distance R between the two interacting molecules, e.g., the shorter incipient interfragment bond, coupled mainly with the CC and OO (or CC) stretchings. The second direction of negative curvature is again the same for both systems and is associated to the opening of the CCOO or CCCC dihedral angle (i.e., a torsion around the shorter incipient CO or CC bond). In the supra–antara saddle point the coordinate R is coupled for both systems with a torsion around the C_2 axis describing a synchronous ring-closure/opening motion (see Figures 1 and 2 of ref 31a and Figures 2–4 from this paper). The second direction of negative curvature is associated with an opening or closure motion of both the CX′X and OXX′ (or CXX′) angles, where X′ and X are the midpoints of the CC and OO (or CC) bonds. In both the supra–antara and syn saddle points and for both systems, the second direction of negative curvature points toward a gauche geometry of C_1 symmetry. The supra–antara structure is located for the O_2 + ethene system just 1 kcal mol^{-1} lower in energy than the supra–supra, but in the ethene dimerization reaction it is much higher than the supra–supra structure. This situation arises in the latter system because of the substantial deformation required to allow an antarafacial involvement of one ethene molecule; the large energy difference makes the supra–supra saddle point a minimum with respect to the supra–antara saddle point along the coordinate pointing from the former to the latter, i.e., the torsional angle Φ. The comparison between the two systems is more complicated when the relationship between the supra–supra and the syn critical points is considered, because of the intersection of the two singlet surfaces in the O_2 + ethene system. For the ethene + ethene system the supra–supra critical point is a maximum with respect to the coordinate pointing from it to the syn critical point, and this feature may be understandable in terms of energy differences: the electron repulsion is lowered by the deformation leading to the syn structure, and the energy drops by ca. 16 kcal mol^{-1}. For the remaining diradical approaches (gauche and anti), the similarities between the two systems are very close. Both show the presence of two first-order saddle points leading to different minima related to stable conformations of the corresponding diradicals. Both reactions are therefore described as two-step, evolving through a gauche-diradical pathway, because the anti conformation of the diradical is connected through the product via the gauche conformation.

Conclusions

The energy hypersurface for the addition reaction of the singlet oxygen molecule to ethene giving dioxetane as product has been studied at the MC–SCF level of theory by two basis sets. The

(31) (a) Bernardi, F.; Bottoni, A.; Robb, M. A.; Schlegel, H. B.; Tonachini, G. *J. Am. Chem. Soc.* **1985**, *107*, 2260–2264. (b) Bernardi, F.; Olivucci, M.; Robb, M. A.; Tonachini, G. *J. Am. Chem. Soc.* **1986**, *108*, 1408–1415. (c) Bernardi, F.; Bottoni, A.; Olivucci, M.; McDouall, J. J. W.; Robb, M. A.; Tonachini, G. *Theochem* **1988**, *165*, 341–351. (d) Bernardi, F.; Olivucci, M.; Bottoni, A.; Robb, M. A.; Schlegel, H. B.; Tonachini, G. *J. Am. Chem. Soc.* **1988**, *110*, 5993–5995.

(32) Dewar, M. J. S. *J. Am. Chem. Soc.* **1984**, *106*, 209–219.

geometries corresponding to critical points on the surface have been fully optimized by gradient methods and characterized by determining the index of the relevant Hessian matrices.

The possibility of three kind of attacks to produce dioxetane has been considered: (1) a concerted [2 + 2] attack of C_{2v} (supra-supra) or C_2 (supra-antara) symmetry; (2) a diradicaloid attack of C_1 (gauche) or C_s (syn or anti) symmetry, which could be concerted (but asynchronous) or not, depending on the existence of diradical minima; (3) an attack leading directly to peroxirane, which could be an intermediate for the reaction leading to dioxetane as final product.

A synchronous concerted path does not exist: both the planar supra-supra approach and the supra-antara approach, obtained from the supra-supra by rotation of O_2 along the C_2 axis, correspond to saddle points of order higher than 1, not related to a transition structure. These points are located ca. 50 kcal mol^{-1} above the dissociation limit with both basis sets.

For a C_s syn approach, having some diradical character, the lowest energy surface corresponds to a singlet state that could be labeled $\Pi 3$ from the occupancy of the π molecular orbitals orthogonal to the molecular symmetry plane. This surface puts the lowest singlet state of the syn-diradical minimum in direct relation to one of the two degenerate singlet states of O_2 (reactants at infinite separation), but it cannot connect the syn $\Pi 3$ saddle point directly with the product dioxetane, whose ground state is $\Pi 4$. Due to the symmetry of the system, these two species are related by a real crossing of the $\Pi 3$ and $\Pi 4$ surfaces. For the same reason a real crossing occurs between the supra-supra critical point and the two syn saddle points that have been found on the $\Pi 3$ and $\Pi 4$ surface. These syn saddle points are both second-order, and the lowest one is located ca. 30 kcal mol^{-1} above the dissociation limit.

Corresponding to a C_1 gauche attack, a first-order saddle point having some diradical character is found. The transition structure is located ca. 29 kcal mol^{-1} above the dissociation limit. Corresponding to this transition structure, a gauche minimum of the peroxy diradical is found. In the gauche attack, the symmetry of the system is lowered and the two electronic states considered above can mix: the system can therefore proceed from the reactants through a C_1-diradical path to the dioxetane minimum in two steps.

A second first-order saddle point is found for a C_s anti approach, leading to another conformational minimum of the peroxy diradical. The barrier height is the same as for the gauche approach. The conformational minima of the peroxy diradical are very close in energy and present a barrier for redissociation of ca. 12 kcal mol^{-1}.

A path leading directly to peroxirane does not appear to exist because the C_s peroxirane-like critical point that has been found is a second-order saddle point. Consequently, the peroxirane minimum (as the dioxetane minimum) seems to be reachable only passing through the gauche-diradical minimum.

Acknowledgment. This work was supported by grants from NATO (RG 096-81) and the NSF (CHE 83-12505 and CHE 87-11901). We thank CSI-Piemonte and Wayne State University for generous allocations of computer time.

Registry No. O_2, 7782-44-7; ethene, 74-85-1.

A Simulation of the Sulfur Attack in the Catalytic Pathway of Papain Using Molecular Mechanics and Semiempirical Quantum Mechanics

Dorit Arad, Robert Langridge, and Peter A. Kollman*

Contribution from the Department of Pharmaceutical Chemistry, University of California, San Francisco, California 94143. *Received August 29, 1988*

Abstract: Recent theoretical studies revealed a unique behavior of the sulfur nucleophile in its attack on formamide, relative to the analogous oxygen reaction. These studies together with experimental evidence suggest that an exact correspondence between the serine and sulfhydryl enzymatic hydrolysis mechanism cannot be made. This prompted us to simulate alternative pathways on the sulfhydryl peptide hydrolysis reaction surface by molecular mechanics and semiempirical quantum mechanical methods in order to attempt to find those that might be in accord with theoretical as well as the experimental results. The molecular mechanics AMBER minimizations of two different enzyme-substrate conformations in papain led to a new conformation which is 29.2 kcal/mol lower in energy then the classic Michaelis complex in which the substrate carbonyl is pointed toward an oxyanion hole. This new conformation is a noncovalent complex between the charged sulfur and a NH bond of the substrate, and is stabilized by electrostatic interactions between sulfur and the substrate. Both Michaelis complexes were used as a basis to construct two tetrahedral covalent structures. The one based on the more stable Michaelis complex was calculated to be more stable by 14.5 kcal/mol. Finally, semiempirical AM1 reaction paths simulations were performed on each of the conformations, simulating the approach of the substrate reactants to the sulfur nucleophile, and the proton-transfer reaction from histidine-159 to the substrate. Our results suggest a new mechanism for papain-catalyzed hydrolysis of peptides, in which a proton transfer from histidine either to oxygen or nitrogen occurs prior to or concerted with the nucleophilic attack. The results suggest reinterpretation of some experimental data and encourage new experiments to test these predictions.

The cysteine proteases constitute a group of endopeptidases whose members owe their catalytic activity to the presence of cysteine and histidine residues in their active site.[1] The three-dimensional structure of the cysteine protease papain has been determined at high resolution using X-ray diffraction by Kamphius et al.[2] who have also proposed a mechanism for the action of papain on the basis of the observed binding of chloromethyl ketone substrate analogues to the enzyme.

The mechanism proposed by these authors is similar to the mechanism of catalysis postulated for the serine proteases.[3] Since

(1) (a) Polgar, L.; Halasz, P. *Biochem. J.* **1982**, *207*, 1-10. (b) Willenbrock, F.; Kowlessur, D.; O'Driscoll, M.; Patel, G.; Quenby, S.; Templeton, W.; Thomas, E. W.; Willenbrock, F. *Biochem. J.* **1987**, *244*, 173-181 and references cited therein.

(2) Kamphuis, G.; Kalk, K. H.; Swarte, B. A.; Drenth, J. *J. Mol. Biol.* **1984**, *179*, 233-256.

0002-7863/90/1512-491$02.50/0